Solar Energy
And Sustainable Development
Refereed, biannual scientific journal issued by:
The Libyan Center for Solar Energy Research and Studies

InGaP/InGaAs/Ge Multi-Junction Solar Cells Efficiency Improvements Using Interposed Transport Layers

Kossivi A. DONKATA[1], Daniel T. COTFAS[2], Petru A. COTFAS[3], Katawoura BELTAKO[4], Milohum M. DZAGLI[5*].

[1,4,5]Laboratoire de physique des Matériaux et des Composants à Semi-conducteurs, University of Lomé, Lomé, Togo.
[1,2,3]Department of Electronics and Computers, Transilvania University of Brasov, Brasov, Romania.
[5]Centre d'Excellence Régional pour la Maîtrise de l'Électricité, University of Lomé, 01BP1515 Lomé1, Togo.

E-*mail:* [5] mdzagli@gmail.com .

ARTICLE INFO.

Article history:
Received 20 Nov 2024
Received in revised form 21 Nov 2024
Accepted 8 Apr 2025
Available online 22 Apr 2025

KEYWORDS

III-V semiconductor, multi-junction solar cell, ETL WS_2, HTL rGO, SCAPS 1D.

ABSTRACT

The high conversion efficiency of solar cells can make them more competitive in cost compared to conventional energy sources. Therefore, enhancing photovoltaic cell efficiency remains a critical challenge for researchers and manufacturers. Shockley-Queisser single junction photovoltaic cells are limited to 33.7% , and multi-junction solar cells are the most promising technologies that have achieved remarkable efficiencies exceeding 46%. Modeling and simulation are essential to optimize semiconductor devices and reduce their development time and cost.

This study investigates the performance improvement of novel InGaP/InGaAs/Ge triple-junction solar cells by integrating III-V semiconductors. The design includes Tungsten disulfide as an electron transport layer, reduced graphene oxide as a hole transport layer, and intrinsic InGaAs layers to improve efficiency in decreasing the number of InGaP, InGaAs, and Ge layers to reduce manufacturing costs. SCAPS 1D software was used to simulate under a solar irradiance of 1000 Wm^{-2} and an air mass of AM1.5G spectrum at 25°C. In addition, a commercial InGaP/InGaAs/Ge solar cell and a mini-solar panel were also simulated, and the obtained current-voltage characteristics were compared with experimental data. A strong correlation was observed between the simulated data and the experimental measurements, confirming the proposed solar cell design's potential, accuracy, and reliability. The new structure produced an impressive power conversion efficiency of 49.83%. The findings suggest a route to manufacturing new multi-junction photovoltaic cells with high efficiency and lower cost.

*Corresponding author.

DOI: https://doi.org/10.51646/jsesd.v14i1.338

تحسينات كفاءة الخلايا الشمسية متعددة الوصلات InGaP/InGaAs/Ge باستخدام طبقات النقل المتداخلة

كوسيفي دومكاتا ، دانيل كوتفاس، كاتاورا بيلتاكو، ميلوهووم دزغلي.

ملخص: زيادة كفاءة الخلايا الشمسية يجعلها أكثر حظا في التنافس في سوق الطاقة. ولذلك، يظل تعزيز كفاءة الخلايا الكهروضوئية تحدياً للباحثين والمصنعين. سجلت كفاءة الخلايا الضوئية أحادية الوصلة 33.7% ، والخلايا الشمسية متعددة الوصلات هي أكثر التقنيات الواعدة التي حققت كفاءة ملحوظة تتجاوزت 46%. تُعد النمذجة والمحاكاة ضرورية لتحسين أجهزة أشباه الموصلات وتقليل وقت تطويرها وتكلفتها. تبحث هذه الدراسة في تحسين أداء الخلايا الشمسية ثلاثية الوصلات InGaP/InGaAs/InGaAs/Ge الجديدة من خلال دمج أشباه الموصلات III-V. ويتضمن التصميم ثاني كبريتيد التنجستن كطبقة ناقلة للإلكترونات، وأكسيد الجرافين المختزل كطبقة ناقلة للثقب، وطبقات InGaAs الجوهرية لتحسين الكفاءة في تقليل عدد طبقات InGaP و InGaAs و Ge لتقليل تكاليف التصنيع. استُخدم برنامج SCAPS 1D لمحاكاة اداء الخلية تحت شدة إشعاع شمسي قدره 1000 واط/م^2 وكتلة هوائية AM1.5 عند درجة حرارة سطح الخلية 25 درجة مئوية. وبالإضافة إلى ذلك، تمت مقارنة خصائص التيار والجهد لخلية شمسية تجارية InGaP/InGaAs/Ge وخلية شمسية صغيرة التي تم الحصول عليها من المحاكاة مع البيانات التجريبية. لوحظ وجود ارتباط قوي بين بيانات المحاكاة والقياسات التجريبية، مما يؤكد إمكانية تصميم الخلية الشمسية المقترحة. من الجدير بالذكر، أن الخلية الجديدة سجلت كفاءة تحويل طاقة مثيرة للإعجاب.

الكلمات المفتاحية – أشباه الموصلات III-V ، خلية شمسية متعددة الوصلات، SCAPS 1D، HTL rGO، ETL WS_2 .

1. INTRODUCTION

The massive use of energy resources accompanies the constantly increasing world population. Global energy demand increases and poses a global warming issue due to the greenhouse gases emitted from the intensive use of fossil fuels [1]. With the scarcity of fossil fuels and climate change concerns, it is crucial to develop new methods and efficient materials for energy production and storage [2], [3], [4],[5]. Significant efforts led to using renewable energy sources for energy production including solar energy as an alternative to fossil fuels [6].

Two main technologies are used in the manufacture of single-junction solar cells namely first-generation and second-generation. The first-generation cell is made of a single crystal structure of silicon wafers at about 300 µm of thickness. It represents approximately 86% of the market of solar cells for applications on Earth [7]. The second generation is constituted of thin films of semiconductor coating layers on different substrates [8]. The introduction of thin films in the solar cell industry led to the production of low-cost cells. Some photovoltaic (PV) cells are still in the research stage while other cells based on silicon (amorphous, polycrystalline, and microcrystalline) are massively produced [8], [9]. The efficiency of about 22.8% of first-generation cells makes up most of the cells on the market. The difference in efficiency decreased over time between the two generations of solar cells and the efficiency of the second generation has taken over [10]. Single-junction solar cell conversion efficiency is limited theoretically at 30% around the 1 eV band gap [11], [12]. This limit is mainly caused by their failure to convert a wide range of solar spectrum [13] and the energy is lost in transmission and heat [14]. Improving the efficiency of solar cells beyond the theoretical limit would help to take greater advantage of the unlimited potential of the sun [15], [16]. Different methods have been addressed over time [17], from single junction to multi-junction [18].

Multi-junction PV cells based on III-V semiconductors are widely explored for space applications [19] and present the highest efficiency [20], [21]. Multi-junction technology uses a wider spectrum of solar energy conversion showing immense improvement in efficiencies of about 35.8% for space and terrestrial applications [22]. This is due to stacking multiple individual semiconductor junctions with various band gaps that absorb a wide range of solar radiation. The choice is made to minimize the losses regarding the thermalization of hot carriers and low-energy photon transmission [23]. Therefore, the photon energy conversion in multi-junction PV cells is more efficient than in single-junction PV cells. Multi-junction PV cells reached a high efficiency and different theoretical models were used to estimate the theoretical conversion efficiency of solar cells [24]. Among the proposed models, the most popular one is the detailed equilibrium limit model based on the laws of thermodynamics. Recently, the conversion limit of different PV cells was calculated using the extended detailed balancing limit, such as solar cells based on quantum dot [25], multi-band [26], and multi-junction [27]. Some authors obtained a maximum conversion efficiency of 86.8% for a multi-junction solar cell, using the detailed equilibrium limit model, with an infinite sub-cell under concentrated light conditions [28]. The high conversion efficiency was 51.2% for the InGaP/GaAs/InGaAs triple junction solar cell under the AM 1.5G, at 289.15 K. The band gap combination used is 1.91/1.37/0.93 eV [25]. Various studies have reported high-efficiency multi-junction solar cells (MJSC) experimentally. For example, an efficiency of 47.1% was reported using the AM 1.5 D spectrum at 143 solar concentrations for III-V six-junction solar cells [29]. An efficiency of 35.9% was reported by Schygulla et al. [30] for III-V/Si triple junction solar cells under AM 1.5 G spectrum. Essig et al. [31] reported at a sunshine concentration, 32.8% and 35.9% efficiencies for a double III-V/Si junction and a three III-V/Si junction solar cells under 1.5G AM illumination, respectively. Aho et al. [32] obtained 39% efficiency for GaInP/GaAs/GaInNsSb/GaInNAsSb solar cells using AM 1.5 D illumination at 560 solar concentrations. Takamoto et al. [33] obtained an efficiency of 44.4% in an InGaP/GaAs/InGaAs triple junction solar cell under AM 15 D illumination at 302 solar concentrations. To date, the efficiency of III-V multi-junction PV cells under non-concentrated (mono-sun) illumination has continued to increase due to the improvement of material quality and the addition of more junctions, which can minimize power losses through thermalization while optimizing the band gap combination. A recent method of incorporating a superlattice of quantum wells (InGaAs/GaAsP) into the central cell of the IMM-3JSC structure solved the current shift problem by confining electrons and holes in a quantum well. This increased optical absorption in the central cell and achieved a record efficiency of 39.5% for hubless applications [34]. Nevertheless, many challenges persist in the evolution and commercialization of MJSC such as the high production costs attributed to the use of high-end materials like gallium arsenide (GaAs). Research has been conducted to tackle the complexities associated with multi-junction PV cells [35], including exploring alternative materials and innovative manufacturing methods to achieve increased efficiency and reduce costs [36]. Furthermore, modeling and simulation techniques have been employed to optimize the efficiency of multi-junction PV. Analytical and numerical methods were combined to simulate the characteristic properties of PV cells, facilitating tailor-made design optimization for specific applications [37][38]. Triple-junction PV cells, with three different semiconductors with various band gaps, have emerged as a leading contender for efficient solar energy conversion [39]. Optimizing their design can further improve efficiency [40]. Through numerical analysis, researchers optimized an InAlAs/InGaAsP/InGaAs triple junction cell to enhance its conversion efficiency by up to 44% [41]. Optimizing the thickness of the absorbing layer and minimizing the charge carrier recombination rates can significantly improve the device efficiency [42]. InGaP/InGaAs/Ge triple-junction solar cells are renowned for their high efficiency in converting solar energy into electricity. Studies refined the design parameters of InGaP/GaAs/Ge triple-junction PV cells through modeling and simulation achieving 36.2% efficiency [43] and improving the efficiency by streamlining its structure to mitigate series resistance [44]. These multi-junction cells have achieved conversion efficiencies of up to 46% [45]. The optimal band gap alignment for improved efficiency is InGaP (1.85 eV bandgap) as the top cell, InGaAs (1.4 eV bandgap) as the middle cell, and Ge (0.67 eV bandgap) as

the bottom cell. This combination allows for better spectrum utilization, reducing thermalization losses and increasing PCE. The robust performance of these materials under varying temperatures and irradiation conditions makes them an ideal choice for MJSC [46].
However, this combination still faces limitations in charge transport, surface recombination losses , and high production costs. To address this, the current research explores reducing the number of layers, such as InGaP, InGaAs, and Ge, by incorporating electron transport layers (ETL) and hole transport layers (HTL). To do this, tungsten disulfide (WS_2) and reduced graphene oxide (rGO) are being investigated to enhance charge extraction and efficiency.
This study aims to evaluate the performance of a novel InGaP/InGaAs/Ge three-junction solar cell using SCAPS-1D and to compare the current-voltage characteristics with the experimental data at three temperatures. Additionally, PV cell and panel parameters were extracted using the Manta Ray Foraging (MRF) algorithm implemented in LabVIEW, with accuracy assessed via root mean square error (RMSE) against other algorithms. The proposed cell structure achieves 49.83% efficiency under natural sunlight at 1 sun by integrating transport layers and reducing the number of layers such as InGaP, InGaAs, and Ge. By refining the capture cross-section, optimizing the thickness, and reducing the defect density, the efficiency reaches 57.60%.

2. MATERIALS AND METHODS

2.1. Material parameters and numerical simulation

The calculations were carried out using SCAPS-1D version-3.3.09 software [46][47] to evaluate the parameters of the PV performance of InGaP/InGaAs/Ge MJSC. This work uses the drift-diffusion method and simulates a multi-junction solar cell (MJSC) composed of InGaP, InGaAs, and Ge. This approach accurately analyzes charge carrier transport, recombination mechanisms, and electric field distribution. The differential equations were solved to determine the current-voltage density curve (J-V). Poisson equation (Eq.1), electronic continuity equation (Eq. 2), and hole equation (Eq. 3) are integrated into the SCAPS-1D software [46][47][48]. These curves are used to calculate the open-circuit voltage (V_{OC}), short-circuit current density (J_{SC}), fill factor (FF), and power conversion efficiency (PCE) of the solar cell device.

$$\frac{d}{dx}\left(-\varepsilon(x)\frac{d\psi}{dx}\right)=q\left[p(x)-n(x)+N_D^+(x)-N_A^-(x)+p_t(x)-n_t(x)\right] \quad (1)$$

$$\frac{dn_p}{dt}=G_n-\frac{n_p-n_{po}}{\tau_n}+n_p\mu_n\frac{dE}{dx}+\mu_n E\frac{dn_p}{dx}+D_n\frac{d^2n_p}{dx^2} \quad (2)$$

$$\frac{dp_n}{dt}=G_p-\frac{p_n-p_{no}}{\tau_p}+p_n\mu_p\frac{dE}{dx}+\mu_p E\frac{dp_n}{dx}+D_p\frac{d^2p_n}{dx^2} \quad (3)$$

Where G_i is the generation rate (electron and hole), τ_n, is the electron lifetime, τ_p , is the hole lifetime, q, is the electron charge, D, is the diffusion coefficient, ε, is the permittivity, μ_n, and μ_p, are the electron and the hole mobilities, $n(x)$ and $p(x)$, are the concentration of free electrons and free holes, $p_t(x)$ and $n_t(x)$, are the concentration of trapped holes and trapped electrons, ψ, is the electrostatic potential, $N_D^+(x)$ and $N_A^-(x)$ are the concentration of ionized acceptors and ionized donors, and E, is the electric field. In addition, x represents the direction of the thickness of the PV cell.
To carry out the extraction of PV parameters for the simulated and real solar cells such as photogenerated current (I_{ph}), saturation current (I_0), ideality factor of diode (n), shunt resistance (R_{sh}), and series resistance (R_s), the Manta Ray Foraging metaheuristic algorithm was implemented

in the LabVIEW program as proposed in reference [49]. Manta Ray Foraging (MRF) is used to solve complex optimization problems in areas like energy optimization, biomedical applications, engineering problems, etc. MRF is a powerful tool for solar energy optimization, improving power conversion, system sizing, microgrid stability, etc. Its effectiveness makes it a promising method for enhancing solar system efficiency and reliability [50][51]. In this algorithm, the equations (4) to (8) were associated to determine these parameters. The output current of the solar cell is calculated as in Eq. (4).

$$I_L = I_{ph} - I_d - I_{sh} \tag{4}$$

Where I_L indicates the output current of the cell, I_d, the diode current, I_{ph} denotes the total current produced by the PV cell, and I_{sh}, the shunt resistor current. According to the Shockley equation, the diode current I_d can be formulated as in Eq.(5).

$$I_d = I_{sd}\left[exp^{\left(\frac{V_l + R_S.I_L}{n.V_t}\right)} - 1\right] \tag{5}$$

Where V_L indicates the cell output voltage and V_t, is the thermal junction voltage defined by Eq.(6).

$$V_t = \frac{KT}{q} \tag{6}$$

Where K is the Boltzmann's constant, T is the junction temperature in Kelvin, and q is the electron's charge. According to Ohm's law, the shunt resistor current is calculated using equation (7).

$$I_{sh} = \frac{V_L + R_S.I_L}{R_{sh}} \tag{7}$$

Using equations (4) to (7), the mathematical equation (8) was obtained to describe the solar cell's single-diode model.

$$I_L = I_{ph} - I_{sd}.\left[exp^{\left(\frac{V_L + R_S.I_L}{n.V_t}\right)} - 1\right] - \frac{V_L + R_S.I_L}{R_{sh}} \tag{8}$$

2.2. InGaP/InGaAs/Ge MJSC

Figure 1 presents two structures of InGaP/InGaAs/Ge multi-junction solar cells investigated in this study. Figure 1A represents the structure of the InGaP/InGaAs/Ge considered as a reference solar cell, which was simulated. The simulation results were compared with the parameters of the cell InGaP(1.86eV)/InGaAs(1.40eV)/Ge(0.67eV) (area 1 cm^2 from SolAero), investigated using the Black Widow Optimization Algorithm (BWOA) and the Chameleon Swarm Algorithm (CSA) as described in the reference [52]. The characteristics of the InGaP/InGaAs/Ge solar cell were investigated under natural sunlight (one sun) at 1000 Wm^{-2} of irradiance and at three temperatures: 41.5°C, 51.3°C, and 61.6°C using the RELab system [53] which consists of myDAQ board, I-V characteristic module, and solar cell module where the InGaP/InGaAs/Ge solar cell was mounted. The last module has a temperature sensor with ±0.5°C accuracy and a high-resolution irradiance sensor that converts the sunlight to frequency [54]. The characteristics of CTJ30 solar cells (area 26.5 cm^2, for CESI) were obtained from the references [52][54][55], using radiation of 1000 W/m^2 and 25°C. Figure 1B corresponds to the proposed InGaP/InGaAs/Ge multi-junction-based PV cell structure with some modifications, showing the details of the layers, their parameters, and thickness.

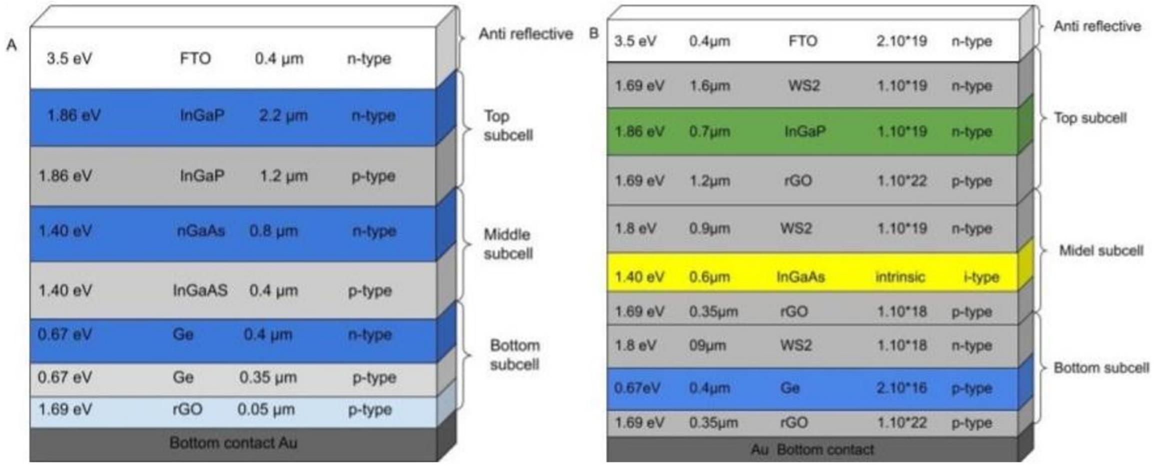

Figure 1. A-Illustration of the 3J InGaP/InGaAs/Ge solar cell. B- Proposed schematic of a multi-junction solar cell based on InGaP/InGaAs/Ge materials.

III-V MJSC, such as six-junction designs, have achieved high efficiencies, with records exceeding 47% under concentrated sunlight [29][56][57]. However, they are expensive due to the high material and manufacturing costs. These cells are mainly used in space applications where efficiency is more critical than cost [35][58]. Researchers are exploring cost-reduction methods, including substrate reuse and integration with material, to make them more viable for terrestrial use [29][59]. An accurate numerical model is essential for deeply understanding the phenomena occurring inside a solar cell [18][57]. The simulation of the reference and the proposed cells was carried out using SCAPS 1D software. Concerning the new proposed structure of the PV cell (Figure 1B), HTL (rGO) and ETL (WS_2) were introduced to encapsulate the absorption layers including the intrinsic layer (InGaAs) [60], [61]. WS_2 is a stable, non-toxic, and eco-friendly n-type semiconductor, making it a great choice as an electron transport layer (ETL) in solar cells. It improves efficiency by enhancing electron transport and reducing energy losses. WS_2 enhances light absorption and charge transport due to its high optical absorption and excellent carrier mobility. WS_2 is chosen for its high charge carrier extraction at solar cell interfaces [62][63]. Similarly, rGO improves conductivity and reduces energy losses, leading to higher efficiency [64]. Together, these materials optimize solar cell performance. rGO is used as a hole transport layer (HTL) due to its tunable work function (4.4–4.9 eV) and good thermal stability [65]. Integrating WS_2 and graphene-based rGO into InGaP/InGaAs/Ge multi-junction cells enhances optical absorption and electrical performance, making it a promising approach for high-efficiency solar cells. Optimizing the thickness and carrier properties of different layers resulted in an appropriate short-circuit current [62][64].

Figure 1B shows that InGaAs composite material is used as an intermediate cell, transport layers of electrons (WS_2) and holes are added between the emitting materials, and the thickness of each layer ranges between 1.6 μm and 0.35 μm. To model the proposed solar cell, the Poisson equation (Eq.1), electronic continuity equation (Eq. 2), and hole equation (Eq. 3) are integrated into the SCAPS-1D software. In this model, physical phenomena such as mobility and the recombination of carriers are calculated. In addition, the impurity rate of the carriers and the thickness are calibrated during the modeling, and the entire simulation is carried out at a temperature of 25 °C. The cell performance is carried out at 1000 Wm^{-2}. The thickness of each layer and the impurity density of carriers were optimized to improve the conversion efficiency. AM1.5G and 1000 Wm^{-2} solar radiation were used to carry out the parameter values, including short circuit current, open circuit voltage, FF, and conversion power at different temperatures and areas.

A statistical test such as the root mean square error (RMSE) is used to assess the accuracy of regression models, as detailed in reference [52]. It quantifies the spread of residuals, i.e., the differences between observed and predicted values, by providing the standard deviation of these residuals. A lower RMSE indicates that the model predictions are, on average, closer to the true values, reflecting better model performance. The model has been proposed considering the material parameters in Table 1.

Table 1. Properties and parameters of the main constituents.

Parameters	Reference materials				Proposed solar cell			
	FTO	InGaP	InGaAs	Ge	FTO	InGaP	InGaAs	Ge
Thickness (μm)	0.4	1.8	2.0	0.4	0,4	0.7	0.6	0.4
Band gap (eV)	3,5	1.86	1.40	0.67	3.5	1.86	1.40	0.67
Electron affinity χ (eV)	4	4.16	3.9	4	4	4.16	3.9	4
dielectric permittivity (relative)	9	11.6	18	16	9	11.6	18	16
Capture cross-section hole (cm^2)	10^{15}	10^{15}	10^{15}	10^{15}	10^{15}	10^{15}	10^{15}	10^{15}
Capture cross section electrons (cm^2)	10^{15}	10^{15}	10^{15}	10^{15}	10^{15}	10^{15}	10^{15}	10^{15}
electron mobility (cm^2/Vs)	1940	1940	20	3900	1940	1940	20	3900
hole mobility (cm^2/Vs)	141	141	20	1900	141	141	20	1900
shallow uniform acceptor density ($1/cm^3$)	0	0	10^{18}	$2\ 10^{15}$	0	0	0	2.10^{16}
Shallow uniform donor density ($1/cm^3$)	10^{15}	10^{16}	0	0	10^{15}	10^{19}	0	0
Defect density Nt($1/cm^3$) uniform	10^{14}	10^{14}	10^{14}	10^{14}	10^{14}	10^{14}	10^{14}	10^{14}

3. RESULTS AND DISCUSSION

3.1. Validations

The reference cell and panel were simulated using SCAPS 1D. The results were compared with the experimental data from [52]. Table 2 presents the external and internal parameters of the reference cell and panel in experimental and simulated cases. The low root mean square errors (RMSE) indicate that the extracted parameters closely match the true values, suggesting a good model fit. RMSE was compared with the results obtained by Cotfas et al. [52] using other algorithms, including the Black Widow Optimization Algorithm (BWOA) and the Chameleon Swarm Algorithm (CSA).

Table 2. Parameters of the experimental and simulation for the panel and three junction solar cells.

Type	Experimental				Simulation			
	Panel	Solar cell	Solar cell	Solar cell	Panel	Solar cell	Solar cell	Solar cell
Temperature (°C)	25	41.5	51.3	61.6	25	41.5	51.3	61.6
Area (Cm^2)	26.5	1	1	1	26.5	1	1	1
I_0 (A)	1.23E-15	3.12E-33	2.57E-31	1.84E-29	3.79E-21	5.16E-26	5.05E-24	5.14E-24
I_{ph} (A)	0.473	0.0121	0.0123	0.0125	0.471	0.0121	0.0126	0.0127

n	2.267	1.321	1.329	1.337	2.357	1.724	1.756	1.678
R_s (Ω)	0.091	1.443	1.411	1.366	0.471	0.595	2.665	2.0675
R_{sh} (Ω)	425.047	275970.19	224268.51	202256.44	6866.58	26501.77	3591.001	17764.77
RMSE	0.0035	7.89E-5	7.56E-5	6.79E-5	0.00012	8.14E-5	8.51E-5	9.06E-5
Algorithms	BWOA	-	-	-	-	8.912E-5	9.451E-5	9.682E-5
	CSA	-	-	-	-	1.018E-4	1.019E-4	5.695E-4

The MRF algorithm showed the highest performance in all three experimental scenarios, thus justifying its adoption for parameter extraction in both experimental and simulated studies. The good match between experimental and simulation cases proves the consistency of the model, showing that it can be successfully used to analyze the newly proposed structure optimized with changes.

Figure 2. presents I-V characteristics under 1000 Wm^{-2} of irradiance for the InGaP/InGaAs/Ge solar panel and PV cells at varying temperatures and surface areas. In all four cases, the I-V characteristics closely matched the experimental data which shows a strong correlation between experimental and simulated data. That indicates that the PV parameters in the simulation model are highly accurate.

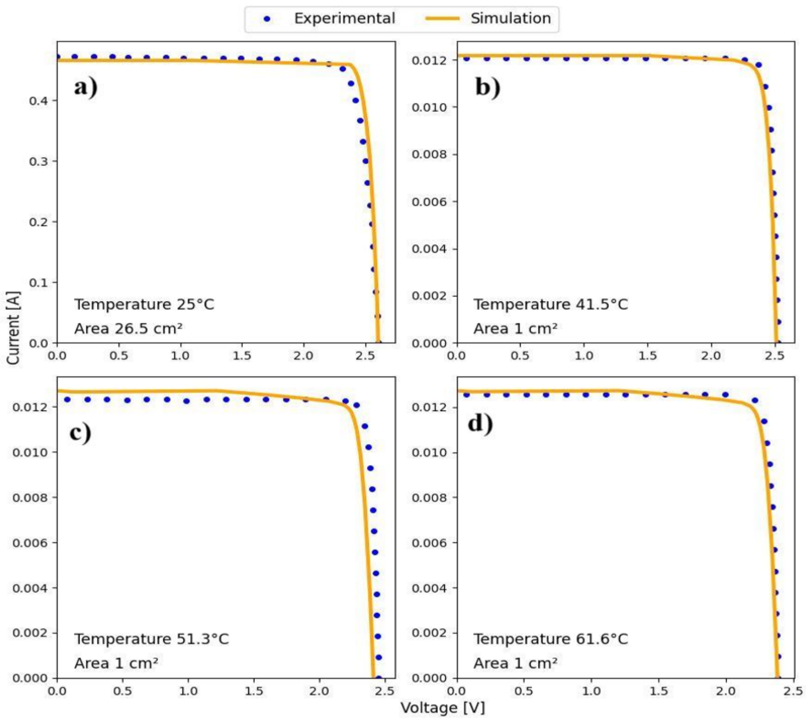

Figure 2. I-V characteristics at 1000 Wm^{-2} : a) solar panel; b) solar cell at 41.5°C; c) solar cell at 51.3°C; d) solar cell at 61.6°C.

This strong agreement confirms the model validation in predicting the behavior of PV cells under different temperatures and surface conditions. As expected, variations in surface area significantly affect the current, while temperature changes exhibit a limited influence on overall performance.

3.2. Analysis of simulation results

The simulation was performed on the proposed PV cell. The simulation results gave a J_{SC} of 20.95 $mAcm^{-2}$, a V_{OC} of 2.66 V, a FF of 89.44%, and a conversion efficiency (η) of 49.83%. In comparison, the simulation of the reference cell exhibited a J_{SC} of 11.80 $mAcm^{-2}$, a V_{OC} of 2.52 V, a FF of 91.51%, and an efficiency of 33.83%. The short-circuit current was increased by about 0.1976 A, the V_{OC} increased by 0.14 V, and the efficiency increased by 16%. Significant improvements were observed in the performance of the proposed cell with some modifications addressed compared to the reference solar cell at the same dimensions of the structure with no integration issues. Figure 3 presents the J-V characteristics of the composed cells.

All the curves illustrate the current distribution among the different sub-cells. The bottom cell, with its lower band gap, exhibits the highest current density (J_{SC} = 57.52 $mAcm^{-2}$) and the lowest V_{OC} (0.47 V). The bottom sub-cell does not limit the current, nor does the middle cell, which also allows a higher current flow. However, the top cell acts as the current-limiting sub-cell among the three [66].

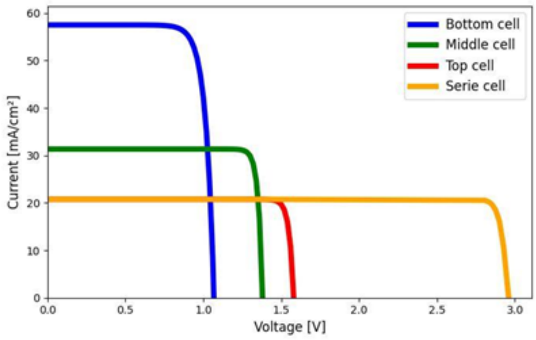

Figure 3. J-V characteristics of sub-cells of the proposed InGaP/ InGaAs/Ge solar cell at 25 °C.

The J_{SC} of the top sub-cell (InGaP) determines the matched current across the series-connected middle (InGaAs) and bottom (Ge) sub-cells. The overall voltage output of the triple-junction cell is the sum of the voltages from the top (InGaP), middle (InGaAs), and bottom (Ge) sub-cells. This cumulative effect results in a total series voltage of approximately 3 V (Figure 3). To optimize the efficiency of a multi-junction solar cell, it is essential to balance the current output from each sub-cell. In this case, the top cell limits the overall current, suggesting that adjustments such as modifying layer thicknesses or tuning the band gaps could help achieve better current matching [67]. By combining materials with different band gaps, MJSC can capture a wider range of the solar spectrum. Each sub-cell absorbs a specific portion of sunlight, minimizing energy losses and improving overall efficiency compared to single-junction cells [58].

The performance of the proposed PV cells was evaluated at four temperatures: 25°C, 41°C, 51.3°C, and 61.6°C, under a solar irradiance of 1000 Wm^{-2} of the AM 1.5 G spectrum. Figure 4 presents the current-voltage characteristics for the InGaP/InGaAs/Ge PV cells. At 25°C (blue curve), the cell performs best, maintaining the highest V_{OC} and a relatively stable current. As temperature increases (41.5°C in red, 51.3°C in green, and 61.6°C in yellow), the V_{OC} decreases, leading to reduced efficiency. At 61.6°C, the performance degradation is most pronounced, as elevated temperatures adversely affect the electrical properties of solar cells, leading to reduced efficiency and output power [68].

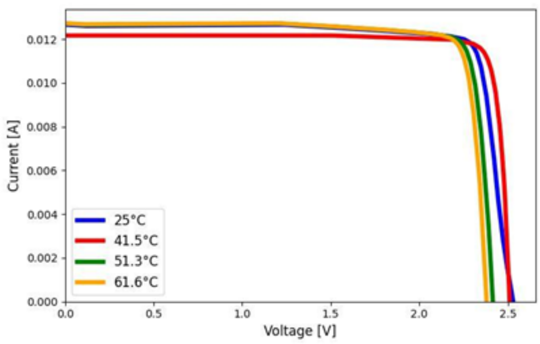

Figure 4. I-V characteristics of the proposed InGaP/ InGaAs/Ge PV cells at different temperatures.

Table 3 presents the calculated parameters of the proposed InGaP/InGaAs/Ge solar cells for different temperature conditions, demonstrating performance improvement compared to previous results [69]. The analysis of the behavior of the obtained parameters shows an increase in the short-circuit current and the FF while the V_{OC} and the efficiency decrease with increasing temperature.

Table 3. Parameters at different temperatures.

	Temperature	V_{OC} (V)	Is (A)	η (%)	FF (%)
Reference	25°C	2.52	0.0118	33.83	91.51
Proposed cell	25°C	2.66	0.2094	49.83	89.44
	41°C	2.62	0.2095	49.21	89.64
	51.3°C	2.59	0.2096	48.76	89.77
	61.6°C	2.56	0.2099	48.18	89.35

These results indicate a slight decrease in efficiency with increasing temperature, a common trend in solar cells. Higher temperatures reduce the V_{OC} and increase recombination losses, negatively impacting overall efficiency. Similar effects have been observed in previous studies where both V_{OC} and the FF decrease as the temperature rises, reducing the efficiency of triple-junction solar cells [70]. However, despite this decline, the 49.83% efficiency at 25°C remains higher than that of many previously reported MJSC [71][72].

3.3. Structural optimization

The capture cross-section, defect density, and thickness of each sub-cell were analyzed to enhance the solar cell's efficiency. Initially, the capture cross-section is set at 10-14 cm^2, and the thickness of i-InGaAs, p-Ge, and n-InGaP is set at 600nm, 400nm, and 700nm, respectively. The overall solar cell efficiency reached 49.83%, with a total J_{SC} of 20.95 mAcm^{-2} and a V_{OC} of 2.66V. The defect density was set at 1014 cm-3. Figure 5 presents the variation of InGaP/InGaAs/Ge solar cell parameters (J_{SC}, V_{OC}, FF, and PCE) as a function of capture cross-section, defect density, and thickness.

Figure 5A shows the variation of PV parameters with the capture cross-section in the n-InGaP, i-InGaAs, and p-Ge layers. It is observed that the efficiency increases significantly as the electron capture cross-section decreases. Figure 5A(d) demonstrates that a smaller capture cross-section reduces recombination losses, which leads to the higher current generation (Figure 5A(b)), the increase of V_{OC} (Figure 5A(a)), and the improvement of the FF (Figure 5A(c)) that ultimately boosted the cell efficiency. The FF is also influenced by the recombination losses.

Figure 5B illustrates the effect of defect density on PV parameters in the base layers. Higher defect densities affect negatively the cell performance. A maximum PCE of 57.58%, with a short-circuit current of 20.95 mAcm^{-2}, a V_{OC} of 2.96 V, and an FF of 92.87%, were achieved at an optimal defect density of 10^{12} cm^{-3}. High defect densities create recombination centers that impede electrons and holes from reaching the electrodes. It reduces the energy conversion efficiency and leads to faster degradation of the PV cells which impacts their lifespan and reliability [73]. Figure 5C presents the thickness's influence on the base layers' performance. J_{SC} (Figure 5C(j)) and V_{OC} (Figure 5C(i)) increase steadily with the thickness up to 1200 nm before decreasing. This suggests that thicker layers absorb more photons which generates more electron-hole pairs and potentially increases J_{SC}. The FF (Figure 5C(k)) and the PCE (Figure 5C(l)) rise with the thickness up to 900 nm but decline slightly beyond that, likely due to charge carriers generated far from the junction traveling longer distances, reducing current and FF [70]. The optimized parameters obtained are hole and electron capture cross-section σ (10^{-18} cm^{-2}), defect density Nt (10^{12} cm^{-3}), and thickness (nm) of 1200, 900, and 400 for InGaP, InGaAs, and Ge, respectively.

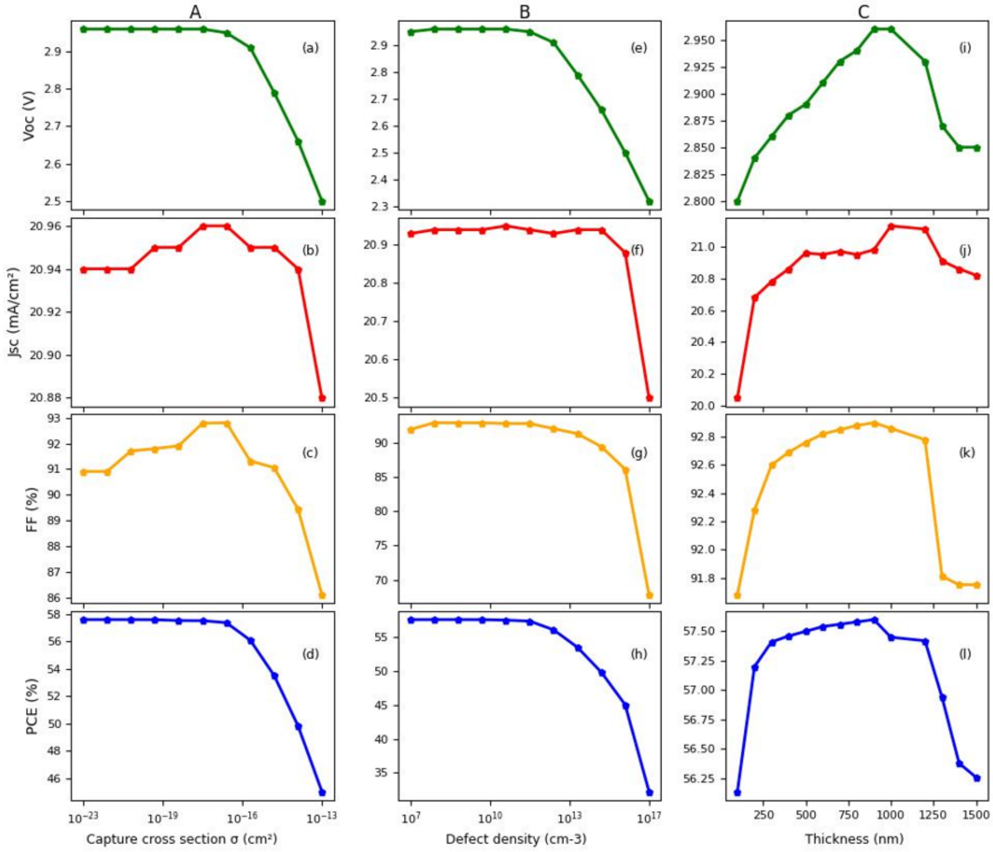

Figure 5. Variation of InGaP/InGaAs/Ge solar cell parameters as a function of A- capture cross-section, B- defect density, and C- thickness.

Figure 6 compares the I-V characteristics of the experimental and the simulated structures for three configurations of a multi-junction solar cell. The blue curve corresponds to experimental measurements, showing an efficiency of 33.83%. It exhibits a lower current density of 0.012 A with a voltage of around 2.5 V. The red curve results from a numerical simulation based on theoretical parameters, achieving an efficiency of 49.83%. Compared to the experimental data, there is a significant improvement, with a higher V_{OC} of 2.7 V and a slightly increased current. The green curve represents an optimized scenario, where parameters such as capture cross-section, layer thickness, and defect density have been adjusted.

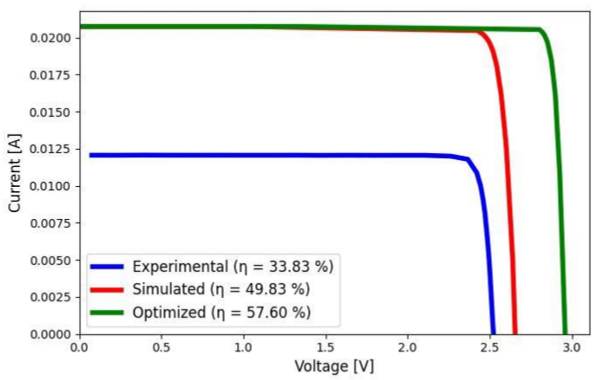

Figure 6. Experimental and simulated I-V characteristics of InGaP/InGaAs/Ge solar cells.

This optimization leads to an efficiency of 57.60% by reducing defects and recombination losses. The maximum performance is reflected in a V_{OC} close to 3 V and a higher current of 0.02 A. This highlights the importance of optimizing key parameters such as capture cross-section, material thickness, and defect density to improve performance. The optimized curve demonstrates that adjusting key parameters can minimize losses and improve current matching between sub-cells. The achieved efficiency of 57.60% surpasses all previously reported efficiencies in MJSC, both in simulations and experimental studies. Table 4 compares the efficiency of solar cells from existing literature with the present findings, clearly demonstrating the high performance of the proposed solar cell.

Table 4. Comparison of estimated 1-sun efficiencies for multijunction solar cells at AM1.5G.

Structure	Spectrum	J_{sc} (mAcm^{-2})	V_{OC} (V)	FF	η(%)	References
GaInP/GaAs/Ge	AM1.5G	14,70	2,69	86,52	34,10	[71]
InGaP/GaAs/InGaAs	AM1.5G	13,47	2,90	82	32,03	[73]
InGaP/InGaAs/Ge	AM1.5G	119,1	2,86	84,0	45,0	[72]
GaInP/GaAs/GaInNAs	AM1.5G	14,70	2,87	84,16	35,50	[34]
GaInP/GaInAs/Si	AM1.5G	12,7	3,309	86,0	36,1	[74]
InGaP/InGaAs/Ge	AM1.5G	2,52	11,8	91,51	33,83	This work
InGaP/InGaAs/Ge	AM1.5G	2,66	20,94	89,44	49,83	This work
InGaP/InGaAs/Ge	AM1.5G	2,96	20,96	92,91	57,60	This work

For context, the National Renewable Energy Laboratory (NREL) previously reported a six-junction solar cell with a record efficiency of 47.1% under concentrated illumination [29]. More recently, a silicon-based multi-junction solar cell achieved an efficiency of 36.1%, marking the highest efficiency for silicon-based cells [21]. Therefore, an efficiency of 57.60% represents a significant advancement beyond these existing records using the proposed configuration. The proposed structure seeks to minimize the use of costly materials like InGaP, InGaAs, and Ge by incorporating more affordable electron and hole transport layers. This strategy enables the development of MJSCs that are cost-effective and highly efficient [74]. By integrating WS_2 and rGO, the model enhances charge carrier mobility, reduces recombination losses, and improves overall stability, providing a significant advantage over traditional designs.

4. CONCLUSION

This study investigates and simulates InGaP/InGaAs/Ge-based solar cells using a model developed in SCAPS-1D, with characteristic parameters extracted via the Manta Ray Foraging Algorithm. Experimental and simulated results show strong agreement, validating the model. WS_2 (electron transport layer) and rGO (hole transport layer) were integrated into the structure to enhance performance and reduce costs. This modification led to a significant efficiency increase from 33.83% to 49.83%, with the optimized design reaching 57.60% through further parameter tuning (capture cross-section, thickness, and defect density). The optimized multi-junction structure demonstrates the potential to overcome the limitations of conventional solar cells by utilizing a broader solar spectrum. This is particularly beneficial for aerospace and dense urban environment applications, where space efficiency is crucial. Replacing expensive materials (InGaP, InGaAs, and Ge) with more cost-effective WS_2 and rGO enables significant cost reductions without compromising performance, promoting the wider adoption of high-efficiency solar technologies. Beyond cost efficiency, WS_2 and rGO offer compatibility with flexible substrates, paving the way for lightweight and flexible solar panels suitable for wearable electronics, smart textiles, and architectural integration (e.g., facades, and windows). In space applications, where multi-junction cells already power satellites, integrating robust materials like graphene could improve performance and durability while reducing payload weight. Furthermore, using sustainable materials and energy-efficient fabrication techniques aligns with global efforts toward eco-friendly PV solutions, minimizing environmental impact. Future research should improve WS_2 and rGO compositions for better charge transport and stability. It should also explore new fabrication methods, develop and test prototypes, and study long-term stability. Cost-effective production techniques and industrial feasibility should also be evaluated. This study outlines a promising approach for achieving high-efficiency, low-cost, and sustainable MJSC, offering broad potential for emerging PV technologies.

Author Contributions: Conceptualization KAD, CDT; Data curation CDT, CPA; Formal analysis CPA, BK, DMM; Investigation KAD, CDT, CPA; Methodology KAD, CDT; Software KAD, CPA; Supervision CDT, BK, DMM; Validation KAD, CDT, CPA; Writing – original draft KAD, CDT; Writing – review and editing KAD, CDT, CPA, BK, DMM.

Funding: This work was supported by "Agence Universitaire de la Francophonie" for the Eugen Ionescu doctoral fellowship and European Union, through the African Research Initiative for Scientific Excellence (ARISE), a pilot program implemented by the African Academy of Sciences [Grant no. DCI-PANAF/2020/420-028].

Data Availability Statement: Not applicable.

Conflict of interest: The authors declare that there is no conflict of interest regarding the publication of this article.

Acknowledgement: The authors thank the "Agence Universitaire de la Francophonie" for the Eugen Ionescu doctoral fellowship that made this research possible. The authors gratefully acknowledge the support of the "Centre d'Excellence Régional pour la Maîtrise de l'Electricité", at the University of Lomé. This document has been produced with the financial assistance of the European Union (Grant no. DCI-PANAF/2020/420-028), through the African Research Initiative for Scientific Excellence (ARISE), pilot program. ARISE is implemented by the African Academy of Sciences with support from the European Commission and the African Union Commission. The contents of this document are the sole responsibility of the author(s) and can under no circumstances be regarded as reflecting the position of the European Union, the African Academy of Sciences, and the African Union Commission.

REFERENCES

[1] Q. Hassan, P. Viktor, T.J. Al-Musawi, B.M. Ali, S. Algburi, H.M. Alzoubi, A.K. Al-Jiboory, A.Z. Sameen, H.M. Salman, and M. Jaszczur, "Renewable energy role in the global energy Transformations", Renewable Energy Focus, Vol. 48, pp. 100545, 2024.

[2] J. Wang, and W. Azam, "Natural resource scarcity, fossil fuel energy consumption, and total greenhouse gas emissions in top emitting countries", Geoscience Frontiers, Vol. 15, no. 2, pp. 101757, 2024.

[3] B.J. van Ruijven, E. De Cian, and I. Sue Wing, "Amplification of future energy demand growth due to climate change", Nature Communications, Vol. 10, no. 1, pp. 2762, 2019.

[4] A. Machín, and F. Márquez, "Advancements in photovoltaic cell materials: Silicon, Organic, and Perovskite Solar cells", Materials, Vol. 17, no. 5, pp. 1165, 2024.

[5] F. Mneimneh, H. Ghazzawi, M. Hejjeh, M. Manganelli, S. Ramakrishna, "Roadmap to Achieving Sustainable Development via Green Hydrogen", Energies, vol. 16, no. 3, p. 1368, 2023.

[6] U.S. Energy Information Administration - EIA, "Carbon dioxide Emissions Coefficient", 2022. Available at: https://www.eia.gov/environment/emissions/co2_vol_mass.php (Accessed: 11 December 2023)

[7] S. Plastras, D. Tsoumatidis, N.D. Skoutas, A. Rouskas, G. Kormentzas, and C. Skianis, "Non-Terrestrial Networks for Energy-Efficient Connectivity of Remote IoT Devices in the 6G Era: A Survey", Sensors, Vol. 24, no. 4, pp. 1227, 2024.

[8] R. Sharma, S. Chuhadiya, M.S. Dhaka, and K. Himanshu, "CdZnTe thin films as proficient absorber layer candidates in solar cell devices: a review", Energy Advances, Vol. 2, pp. 1980-2005, 2023.

[9] N. Wang, F. Meng, L. Zhang, and Z. Liu. "Light soaking of hydrogenated amorphous silicon: a short review", Carbon Neutrality, Vol. 3, no. 1, pp. 18, 2024.

[10] J. Pastuszak, P. Wegierek, "Photovoltaic cell generations and current research directions for their development", Materials, Vol. 15, no. 16, pp. 5542, 2022.

[11] S. Ullah, A. Gulnaz, and G.W. Wang, "Modeling and Simulation of Heterojunction Solar Cell with Mono Crystalline Silicon", Journal of Applied Mathematics and Physics, Vol. 12, no. 3, pp. 997-1020, 2024.

[12] A.D. Dhass, D. Patel, and B. Patel, "Estimation of power losses in single-junction gallium-arsenide solar photovoltaic cells", International Journal of Thermofluids, Vol. 17, pp. 100303, 2023.

[13] A.Y. Alsalloum, B. Turedi, K. Almasabi, X. Zheng, R. Naphade, S.D. Stranks, O.F. Mohammed, and O.M. Bakr, "22.8%-Efficient single-crystal mixed-cation inverted perovskite solar cells with a near-optimal bandgap", Energy & Environmental Science, Vol. 14, no. 4, pp. 2263-2268, 2021.

[14] S.M. Uddin, M.I.A. Bakar, and M.H.H. Mohd Rozlan, "Investigation of Multi-Junction GaInP/GaInAs/Ge Solar Cells Performance Characteristics using MATLAB Simulation", Paper presented at ICE2T 2023 – 4th edition. Proceedings of the 2023 International Conference on Engineering Technology and Technopreneurship (ICE2T), Vol. 15, no. 16, pp. 360-365, August, 2023.

[15] M.B. de la Mora, O. Amelines-Sarria, B.M. Monroy, C.D. Hernández-Pérez, and J.E. Lugo, "Materials for downconversion in solar cells: Perspectives and challenges", Solar Energy Materials and Solar Cells, vol 165, pp. 59-71, 2017.

[16] P. Subudhi, and D. Punetha, "Pivotal avenue for hybrid electron transport layer-based perovskite solar cells with improved efficiency", Scientific Reports, Vol. 13, no. 1, pp. 19485, 2023.

[17] R.M. France, J. Geisz, T. Song, W. Olavarria, M. Young, A. Kibbler, and M.A. Steiner, "Triple-junction solar cells with 39.5% terrestrial and 34.2% space efficiency enabled by thick quantum well superlattices", Joule, Vol. 6, no. 5, pp. 1121-1135, 2022.

[18] D. Kumar, N. Kumar, and L. Kumar, "Impact of operating temperature and solar concentration on the conversion efficiency of InGaP/InGaAs/Ge hybrid triple-junction solar cell", Brazilian Journal of Physics, Vol. 53, no. 1, pp. 31 2023.

[19] A. Baiju, and M. Yarema, "Status and challenges of multi-junction solar cell technology", Frontiers in Energy Research, Vol. 10, pp. 971918, 2022.

[20] A.A. Abushattal, A.G. Loureiro, and N.E.I. Boukortt, "Ultra-High Concentration Vertical Homo-Multijunction Solar Cells for CubeSats and Terrestrial Applications", Micromachines, Vol. 15, no. 2, pp. 204, 2024.

[21] P. Schygulla, R. Müller, O. Höhn, M. Schachtner, D. Chojniak, A. Cordaro, S. Tabernig, B. Bläsi, A. Polman, G. Siefer, D. Lackner, and F. Dimroth, "Wafer-bonded two-terminal III-V//Si triple-junction solar cell with power conversion efficiency of 36.1 % at AM1.5G", Progress in

Photovoltaics: Research and Applications, Vol; 33, no. 1, pp.100-108, 2025.

[22] M.A. Green, E.D. Dunlop, M. Yoshita, N. Kopidakis, K. Bothe, G. Siefer, D. Hinken, M. Rauer, J. Hohl-Ebinger, X. Hao, et al. "Solar cell efficiency tables (Version 64)", Progress in Photovoltaics: Research and Applications, Vol. 32, no. 7, pp. 425-441, 2024.

[23] D.O. Nielsen, C.G. Van de Walle, S.T. Pantelides, R.D. Schrimpf, D.M. D.M. Fleetwood, and M.V. Fischetti, "First-principles approach to closing the 10–100 eV gap for charge-carrier thermalization in semiconductors", Physical Review B, Vol. 108, no 15, p. 155203, 2023.

[24] B. Amiri, and A. Belghachi, "First-principles investigation of absorption coefficient in quantum well designed for solar cells", Optik, Vol. 202, pp. 163554, 2020.

[25] A. Sahu, K. Hiremath, and A. Dixit, "Limiting efficiency factors and their consequences on quantum dot sensitized solar cells: a detailed balance study", Applied Physics A, Vol. 124, pp. 1-8, 2018.

[26] A.S. Brown, and M.A. Green, "Detailed balance limit for the series-constrained two-terminal tandem solar cell", Physica E: Low-dimensional Systems and Nanostructures, Vol. 14, no. 1-2, pp. 96-100, 2002.

[27] S. Abdul Hadi, E.A. Fitzgerald, and A. Nayfeh, "Theoretical efficiency limit for a two-terminal multi-junction "step-cell" using detailed balance method", Journal of Applied Physics, Vol. 119, no. 7, pp. 073104, 2016.

[28] K. NNguyen-Vinh, S. Gonapaladeniya, N. Nguyen-Quang, and Z. Leonowicz,"A Review of Photovoltaic Technology", In : 2024 24th International Scientific Conference on Electric Power Engineering (EPE). IEEE, p. 1-6, 2024.

[29] J.F. Geisz, R.M. France, K.L. Schulte, M.A. Steiner, A.G. Norman, H.L. Guthrey, M.R. Young, T. Song, and T. Moriarty, "Six-junction III–V solar cells with 47.1% conversion efficiency under 143 Suns concentration", Energy, Vol. 5, no. 4, pp. 326-335, 2020.

[30] P. Schygulla, R. Müller, D. Lackner, O. Höhn, H. Hauser, B. Bläsi, F. Predan, J. Benick, M. Hermle, S.W. Glunz, and F. Dimroth, "Two-terminal III–V//Si triple-junction solar cell with a power conversion efficiency of 35.9% at AM1. 5g" Progress in Photovoltaics: Research and Applications, Vol. 30, no. 8, pp. 869-879, 2022.

[31] S. Essig, C. Allebé, T. Remo, J.F. Geisz, M.A. Steiner, K. Horowitz, L. Barraud, J.S. Ward, M. Schnabel, A. Descoeudres, et al. "Raising the one-sun conversion efficiency of III–V/Si solar cells to 32.8% for two junctions and 35.9% for three junctions", Nature Energy, Vol. 2, no. 9, pp. 1-9, 2017.

[32] A. Aho, R. Isoaho, M. Raappana, T. Aho, E. Anttola, J. Lyytikäinen, A. Hietalahti, V. Polojärvi, A. Tukiainen, J. Reuna, et al. "Wide spectral coverage (0.7–2.2 eV) lattice-matched multijunction solar cells based on AlGaInP, AlGaAs, and GaInNAsSb materials", Progress in Photovoltaics: Research and Applications, Vol. 29, no. 7, pp. 869-875, 2021.

[33] V.K. Sharma, E.A. Kumar, and S.S. Murthy, "Influence of dynamic operating conditions on the performance of metal hydride-based solid sorption cooling systems", International Journal of Hydrogen Energy, Vol. 40, no. 2, pp. 1108-1115, 2015.

[34] V. Thakur, B.M. Yu Jeco-Espaldon, and Y.Okada, "Luminescent coupling effect in InGaP/GaAs/InGaAs inverted metamorphic triple-junction solar cell", Journal of Photonics for Energy, Vol. 14, no. 1, pp. 015503-015503, 2024.

[35] M. Yamaguchi, F. Dimroth, J.F. Geisz, N.J. Ekins-Daukes, "Multi-junction solar cells paving the way for super-high efficiency", Journal of Applied Physics, Vol. 129, no. 24, pp. 240901, 2021.

[36] L. Boucerredj, "Modélisation et simulation d'un système photovoltaïque par la commande MPPT", Algerian Journal of Engineering Architecture and Urbanism, Vol. 5, no. 5, pp. 197-205, 2021.

[37] K.G. Beepat, D.P. Sharma, A. Mahajan, D. Pathak, V. Kumar, "Simulation of multijunction solar cell interfaces for enhancement of the power conversion efficiency", Discover Applied Sciences, Vol. 6, no. 6, pp. 1-19, 2024.

[38] X. Zhang, S. Huang, J. Liu, K. Lin, Y. Wang, and W. Yang, Research on monolithic AlGaInP/AlGaInAs/GaInAs/Ge quadruple-junction solar cell for high efficiency lattice-matched tandem photovoltaic device. Applied Physics Express, vol. 13, no 7, pp. 071002, 2020.

[39] D. Sharma, R. Mehra, and B. Raj, "Methods for Integration of III-V Compound and Silicon Multijunction for High Efficiency Solar Cell Design", Silicon, Vol. 14, no. 15, pp. 9797-9804, 2022.

[40] O.A. Al-Shahri, F.B. Ismail, M.A. Hannan, M.S. Hossain Lipu, A.Q. Al-Shetwi, R.A. Begum, N.F.O. Al-Muhsen, and E. Soujeri, "Solar photovoltaic energy optimization methods, challenges and issues: A comprehensive review", Journal of Cleaner Production, Vol. 284, pp. 125465, 2021.

[41] K. Dasgupta, A. Mondal, S. Ray, U. Gangopadhyay, "Mathematical modeling of a novel heterojunction SIS front surface and interdigitated back-contact solar cell", Journal of Computational Electronics, Vol. 20, 5, pp. 1779-1806, 2021.

[42] O. Richard, A. Turala, V. Aimez, M. Darnon, and A. Jaouad, "Low-Cost Passivated Al Front Contacts for III-V/Ge Multijunction Solar Cells", Energies, Vol. 16, no. 17, pp. 6209, 2023.

[43] M.H. Tsutagawa, and S. Michael, "Sherif. Triple junction InGaP/GaAS/Ge solar cell optimization: the design parameters for a 36.2% efficient space cell using Silvaco ATLAS modeling & simulation". In : 2009 34th IEEE Photovoltaic Specialists Conference (PVSC). IEEE, p. 001954-001957, 2009.

[44] A.K. Hamid, N.T. Mbungu, A. Elnady, R.C. Bansal, A.A. Ismail, and M.A. AlShabi, "A systematic review of grid-connected photovoltaic and photovoltaic/thermal systems: Benefits, challenges and mitigation", Energy & Environment, Vol. 34, no. 7, pp. 2775-2814, 2023.

[45] K. Araki, Y. Ota, H. Saiki, H. Tawa, K. Nishioka, and M. Yamaguchi, "Super-multi-junction solar cells—device configuration with the potential for more than 50% annual energy conversion efficiency (non-concentration)", Applied Sciences, Vol. 9, no. 21, pp. 4598, 2019.

[46] M. Burgelman, K. Decock, S. Khelifi, A. Abass, "Advanced electrical simulation of thin film solar cells", Thin Solid Films, Vol. 535, pp. 296–30, 2013.

[47] P. Calado, I. Gelmetti, B. Hilton, M. Azzouzi, J. Nelson, and P.R.F. Barnes, "Diffusion: an open-source code for simulating ordered semiconductor devices with mixed ionic-electronic conducting materials in one dimension", Journal of Computational Electronics, Vol. 21, pp. 960–991, 2022.

[48] S. Karthick, S.Velumani, and Bouclé, Experimental and SCAPS simulated formamidinium perovskite solar cells: A comparison of device performance. Solar Energy, vol. 205, pp. 349-357, 2020.

[49] E.H. Houssein, G.N. Zaki, A.A.Z. Diab, and E.M. Younis, "An efficient Manta-Ray Foraging Optimization algorithm for parameter extraction of a three-diode photovoltaic model", Computers & Electrical Engineering, Vol. 94, pp. 107304, 2021.

[50] A. Zhao, Y. Wang, and L. Chen, "MRFO: A novel metaheuristic algorithm for global optimization," IEEE Access, vol. 8, pp. 12345–12358, 2020.

[51] H. Zhang, X. Li, and P. Kumar, "Application of MRFO in energy-efficient system design," IEEE Transactions on Industrial Electronics, vol. 68, no. 7, pp. 5678–5689, 2021.

[52] D.T. Cotfas, M. Madhiarasan, P.A. Cotfas, "Extraction of the multijunction solar cell parameters using two metaheuristic algorithms", IEEE Access, Vol. 12, pp. 109634-109656, 2024.

[53] P.A. Cotfas, D.T. Cotfas, "Design and implementation of RELab system to study solar and wind energy", Measurement, Vol. 93, no. 94-101, 2016.

[54] F.F. Muhammadsharif, "A new simplified method for efficient extraction of solar cells and modules parameters from datasheet information", Silicon, Vol. 14, no. 6, pp. 3059-3067, 2022.

[55] Thin Triple-Junction Solar Cell for Space Applications, 2020, [online] Available:

https://www.cesi.it/app/uploads/2020/03/Datasheet-CTJ30-Thin.pdf

[56]T. Bidaud, F. Ayari, P. Ferreol, C. Jouanneau, A. Turala, S. Moreau, M. Volatier, V. Aimez, S. Fafard, A. Jaouad, M. Darnon, and G. Hamon, "Multi-Terminal GaInP/GaInAs/Ge Solar Cells for Subcells Characterization". Energies, vol. 17, no. 11, 2538, 2024.

[57] S.S. Soley and A.D.D. Dwivedi, "Numerical simulation and performance analysis of InGaP, GaAs, Ge single junction and InGaP/GaAs/Ge triple junction solar cells", Materials Today: Proceedings, Vol. 39, Part 5, pp. 2050-2055,2021

[58] Z. Ziani, M. Y. Mahdad, M. Z. Bessenouci, M.C. Sekkal, and N. Ghellai, "Enhancing Multi-Junction Solar Cell Performance: Advanced Predictive Modeling and Cutting-Edge CIGS Integration Techniques", Energies, Vol. 17 no.18, p.4669, 2024.

[59] W. Zhao, N. Yang, J. Li, L. Fang, W. Han, W. Lv, M. Yin, and J. Zhang, "Practical Verification and Comparative Analysis of One- and Two-Diode Models of Space Triple-Junction InGaP2/InGaAs/Ge Solar Cell". Journal of Electronic Materials, Vol. 52, pp. 2580–2586, 2023.

[60] A.G. Martin, D.D. Ewan, Y. Masahiro, K. Nikos, B. Karsten, S. Gerald, H. David, R. Michael, H. Jochen, and H. Xiaojing, "Solar cell efficiency tables (Version 64)", Progress in Photovoltaics: Research and Applications, Vol. 32, no. 7, pp. 425-441, 2024.

[61] A. Sahu, K. Hiremath, and A. Dixit, "Limiting efficiency factors and their consequences on quantum dot sensitized solar cells: a detailed balance study" Applied Physics A, Vol. 124, pp. 1-8, 2018.

[62] J. Liu, X. Wang, and Y. Chen, "Tungsten disulfide (WS_2) for stable and efficient perovskite solar cells," IEEE Transactions on Nanotechnology, vol. 21, pp. 233–240, 2023.

[63] S. K. Sharma, P. K. Singh, and S. Islam, "Enhanced charge transport in perovskite solar cells using WS_2 as an electron transport layer," IEEE Journal of Photovoltaics, vol. 11, no. 3, pp. 456–462, 2022..

[64] Y. Zhang, Y. Wang, S. Liu, and J. Wu, "Reduced graphene oxide (rGO) as an efficient charge transport material in solar cells," J. Mater. Chem. A, vol. 8, no. 24, pp. 12056-12073, 2020.

[65] A. Smith, B. Johnson, and C. Lee, "Thermal stability of reduced graphene oxide in photovoltaic applications," Solar Energy Mater. Sol. Cells, vol. 95, no. 5, pp. 1321-1327, 2019.

[66] N. Shrivastav, J. Madan, M.K. Hossain, M.D. Albaqami, and R. Pandey, "Design and simulation of three-junction all perovskite tandem solar cells: A path to enhanced photovoltaic performance", Materials Letters, Vol. 362, no. 136169, 2024.

[67] M.A. Green, E.D. Dunlop, G. Siefer, M. Yoshita, N. Kopidakis, K. Bothe, X. Hao, "Solar cell efficiency tables (Version 61)", Progress in Photovoltaics: Research and Applications, vol. 31, no 1, p. 3-16, 2023,.

[68] Shaker, L.M., Al-Amiery, A.A., Hanoon, W. K. Al-Azzawi, and A. A.H. Kadhum, "Examining the influence of thermal effects on solar cells: a comprehensive review", Sustainable Energy Research,

Vol. 11, p. 6, 2024.

[69] F. Dhiabi, O. Benelmir, and A. Saadoune, "Studying the effects of temperature on InGaP/InGaAs/Ge triple junction solar cells using PyAMS Software". Studies in Engineering and Exact Sciences, vol. 5, no 2, pp. e11388-e11388, 2024.

[70] L.M.N. Nieto, J.P.F. Rodríguez, R.M, Campos, and P.J.P. Higueras. "Multi-junction solar cell measurements at ultra-high irradiances for different temperatures and spectra", Solar Energy Materials and Solar Cells, Vol. 266, pp. 112651, 2024.

[71] J.F. Geisz, R.M. France, K.L. Schulte, M.A. Steiner, A.G. Norman, H. L.Guthrey, and T. Moriarty, "Six-junction III–V solar cells with 47.1% conversion efficiency under 143 Suns concentration", Nature energy, Vol, 5 no. 4, pp. 326-335, 2020.

[72] A.W. Bett, F. Dimroth, W. Guter, R. Hoheisel, E. Oliva, S.P. Philipps and G. Strobl, "Highest efficiency multi-junction solar cell for terrestrial and space applications", Vol. 25(25.8), 30-6, 2009.

[73] S. Ammi, L. Chenini, and A. Aissat, "Impact of InGaAs Thickness and Indium Content on the Performance of (InP/InGaAs/InAlAs) MOSFET Structure", In Proceedings of the 2nd International Conference on Electronic Engineering and Renewable Energy Systems: ICEERE 2020, Vol. 13-15 April Saidia, Morocco pp. 347-352, 2021.

[74] Koga, M., Shibui, S., Matsuoka, N., Sudo, T., & Uchida, S. "Conversion Efficiency of 45.0% in InGaP/InGaAs/Ge Triple-Junction Solar Cells for Laser Power Beaming", Energies, vol. 17, no 13, p. 3299, 2024.

[75] I.M. Peters, C.D. Rodríguez Gallegos, L. Lüer, J.A. Hauch, C.J. Brabec, "Practical limits of multijunction solar cells", Progress in Photovoltaics: Research and Applications, Vol. 31, n. 10, 1006-1015, 2023.